Measurement of the charge-transfer rate of Fe^{3+}-ion coefficients with H_2 and N_2 at electron-volt energy

Kelin Gao,[1,*] Zongxiu Nie,[1] Yurong Jiang,[1,2] and Jiaomei Li[1]

[1]*Laboratory of Magnetic Resonance and Atomic and Molecular Physics, Wuhan Institute of Physics and Mathematics,*
The Chinese Academy of Sciences, P.O. Box 71010, Wuhan 430071, People's Republic of China
[2]*Department of Optical Engineering, Beijing Institute of Technology, Beijing 100081, People's Republic of China*

The charge-transfer rate coefficients of Fe^{3+} with H_2 and N_2 are measured by using a laser-ablation ion source and a quadrupole *radio-frequency* ion trap with the mean collision energy of about 5.1 eV. The rate coefficients for Fe^{3+} with H_2 at the equivalent temperature 1.7×10^3 K and Fe^{3+} with N_2 at 1.3×10^4 K are $1.64(0.22) \times 10^{-10}$ cm^3 s^{-1} and $4.36(0.46) \times 10^{-9}$ cm^3 s^{-1}, respectively. The measured values are of the same order as the Langevin rate coefficient.

PACS number(s): 34.70.+e, 32.80.Pj, 52.50.Jm

I. INTRODUCTION

The process related to multiple-charge ions is one of the fundamental atomic processes in both astrophysical and laboratory plasmas [1]. The multiply charged iron ions are of considerable interest, since they exist practically in every astrophysical object as well as in fusion plasma. It has found that a K_α emission from a multicharged iron ion is most likely the origin of x-ray emission from the central region of the Galaxy [2]. The cross sections for the $3S^2 \, 3P^5 \, ^2P^0_{3/2} - 3S^2 \, 3P^5 \, ^2P^0_{1/2}$ transition in Fe^{9+} have been measured via a 14.0 GHz electron-cyclotron resonance ion source [3]. Distorted-wave calculations have also been carried out for single ionization cross sections of Fe^{q+} in all charged states [4]. Several electron-capture cross-section measurements for ionization of Fe^{q+} ions (q=1 [5], 2 [5,6], 3-4 [5], 5-6, 9, [5,7], 11,13 [8], 15 [8,9]) by electron impact have been performed as well.

However, most of these previous works have focused on collision energies of the KeV order while the collisions with energies of the electron-volt (eV) order play an important role in some processes such as collisions involving multiply charged even high-Z metallic impurities (Fe, Mo, W, Ti) in fusion plasma [10]. These impurities could be produced and released from materials of the wall limiters and reactor of some fusion apparatus in which the charge-transfer process between those ions and neutral atoms or molecules crucially affect the charge- and excitation-state distribution and radiation losses. Little attention has been paid to the electron capture of multiply charged ions and neutral species particularly at electron-volt energies and low charge states which are pronounced at or near the edges of fusion apparatuses. Recently, Kwong introduced a novel technique that is particularly suitable for dealing with the collisions in this low-energy range [11]. With the help of this technique, the charge-transfer rate coefficients between W^{2+}, Mo^{6+}, and Ar have been studied in a cylindrical radio frequency (rf) trap [12,13]. Based upon our experiment of charge transfer

of Ti^{4+} with Ar and N_2 [14], we measured the charge-transfer rate coefficients of Fe^{3+} (average energy of about 5.1 eV) with H_2 and N_2. Our experiment has been performed in a quadrupole rf ion trap, the low-energy Fe^{3+} has been created and then confined in the trap by a laser ablation combined with the technique of crossed-beam cooling for ions.

II. EXPERIMENTAL PROCEDURE

Our experimental apparatus is the same as the one utilized in our previous work [14,15] and consists of a quadrupole rf ion trap with a minimum radius of the ring electrode $r_0 = 0.99$ cm, and the minimum separation between two end-cap electrodes $2z_0 = 1.4$ cm. The trapping parameters (rf frequency $f = 1.1$ MHz, the amplitude rf voltage $V_{AC} = 176$ V) of the quadrupole rf ion trap are chosen to optimize the storage times of Fe^{3+} ions. The axial potential-well depth is $D_z = (e V_{AC}^2 / 4 m z_0^2 \Omega^2) = 17$ V [16]. The arrangement of the apparatus, the method of laser-ablation, and crossed-beam cooling for creating low-energy multicharged ions are similar to those demonstrated in Ref. [11]. Two solid *cast-iron* (99.9% purity) targets are held in the equatorial plane of the ring electrode and at equally fixed distances from its center. We have compared cast irons with pure irons and found that *cast-iron* targets give a more stable ion signal than pure-iron targets. The second harmonic (532 nm) output of a pulsed Nd: YAG laser (power ~ 5 mJ with a pulse duration of ~ 7 ns) is used as the ablation source and split by a 50:50 dielectric-coated beam splitter. The pulse power density is estimated to be greater than 1×10^9 W cm^{-2}. The two pulsed laser beams are collimated and passed through holes in the ring electrodes to strike the target surfaces. Each beam is focused by convex lens with focal length of 50 cm. The ablation plasma beams enter the trap through holes and intersect each other at right angles at the center of the ion trap. A few ions in one beam undergo collisions with ions from the other beam. And some of the scattered ions remain inside the trap for lose almost all their kinetic energy, while others leave the trap for approximately double theirs. Plenty of Fe^{3+} as well as other charge-state ions, such as C^{2+} ($m/q = 6$), C^+ ($m/q = 12$), C_2^+ ($m/q = 24$),
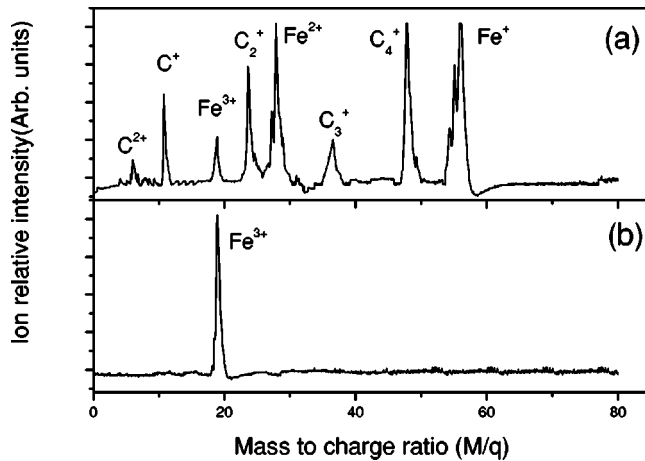
*E-mail address: klgao@wipm.ac.cn

FIG. 1. Mass spectrum of produced ions by laser ablation of the *cast-iron* targets (a) Full spectrum. (b) Selective storage of Fe^{3+} ions. The ion signals in (a) and (b) are not on the same scale.

Fe^{2+} ($m/q=28$), C_3^+ ($m/q=36$), C_4^+ ($m/q=48$), and Fe^+ ($m/q=56$) are produced and confined in the trap [as shown in Fig. 1(a)]. Operating near the cross points of $\beta_z=1$ and $\beta_r=0$ ($V_{AC}=176$ V, $V_{DC}=16.9$ V) in the first stability region of the rf trap, Fe^{3+} ions are selected. Other ions are excluded from the trap, because their orbits are outside the stable region of the trap. These selected Fe^{3+} ions are stored by setting the dc voltage V_{DC} to zero [as shown in Fig. 1(b)]. The timing diagram for production, trapping, and detection of the ions is shown in Fig. 2. Changing the axial instability by increasing the rf voltage applied to the ring electrode along the $a_z=0$ line, the ions are extracted from the trap axially and ejected through a hole in the center of an endcap electrode to the surface of a channel electron multiplier (CEM) quite near the endcap electrode. With an appropriate rf voltage scanning rate (corresponding to a mass scanning rate of about 2000 amu/s), we can obtain the best mass resolution of $M/dM \geqslant 6$ at 12 amu.

The ground-state energy of Fe^{3+} with the electron configuration $3d^5(^6S_{5/2})$ is 30.64 eV. There are some low-lying metastable states $3d^5\,^4G$, $3d^5\,^4P$, $3d^5\,^4D$, whose energies
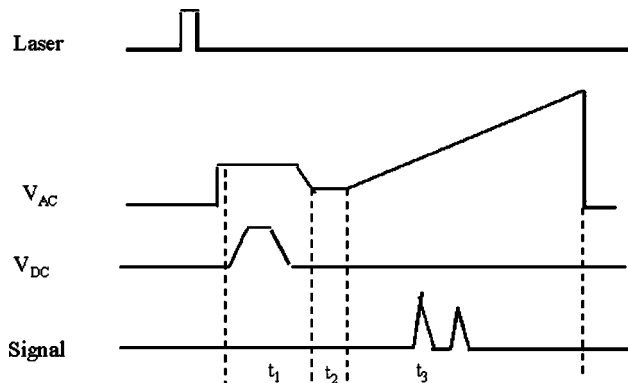

FIG. 2. Timing diagram for ion trap and laser ablation. The voltages of V_{AC} and V_{DC} are selected for mass-selective storage of the Fe^{3+} ions. The delay time from the end of the selective-storage operation to the beginning of the analytical scan can be varied.
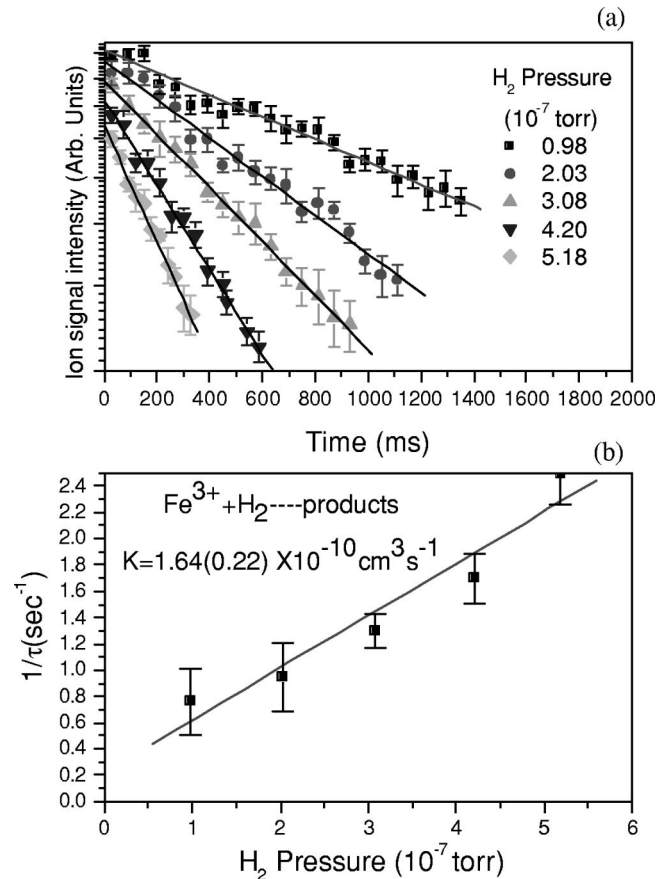

FIG. 3. (a) The decay of relative ion numbers of Fe^{3+} vs storage time in different H_2 pressures. The solid lines are the least-square fits to a single exponential function. (b) Variations of the Fe^{3+} decay rate vs H_2 pressure. The slope of the straight line fit gives the charge-transfer rate coefficient.

shift up 4 eV, 4.4 eV, 4.8 eV from the ground-state energy [17]. Fe^{3+} ions can be in a variety of excited electronic states immediately after they are produced by laser ablation. The excited states are rapidly cascaded to the ground and low-lying metastable states through allowed transitions and collisional deexcitations by the plasma electrons. Using the density and temperature of the laser-induced plasma [18], the ratio of the metastable-state to the ground-state population of Fe^{3+} could be crudely estimated to be small. The population ratio will decrease further due to plasma expands and cross-beam cooling. When we began the measurement (>50 ms late after the ions were produced and selectively trapped), the population ratio drops beyond the observable limit of the current facility. From the observation of a single exponential decay curve of the Fe^{3+} ion signals in Figs. 3(a) and 4(a), we affirmed that the Fe^{3+} ions produced by laser ablation and stored in our trap are essentially in ground state.

The experimental procedure is summarized as follows. The whole vacuum chamber is connected to a JBY—100 ion pump to maintain its ultrahigh vacuum (the residual background pressure is less than 1×10^{-9} torr). Ultrahigh purity reactant gases (99.99%) H_2 and N_2 enter into the vacuum chamber through a gas handling system. The reservoir system is first evaluated to 10^{-7} torr though a molecular pump
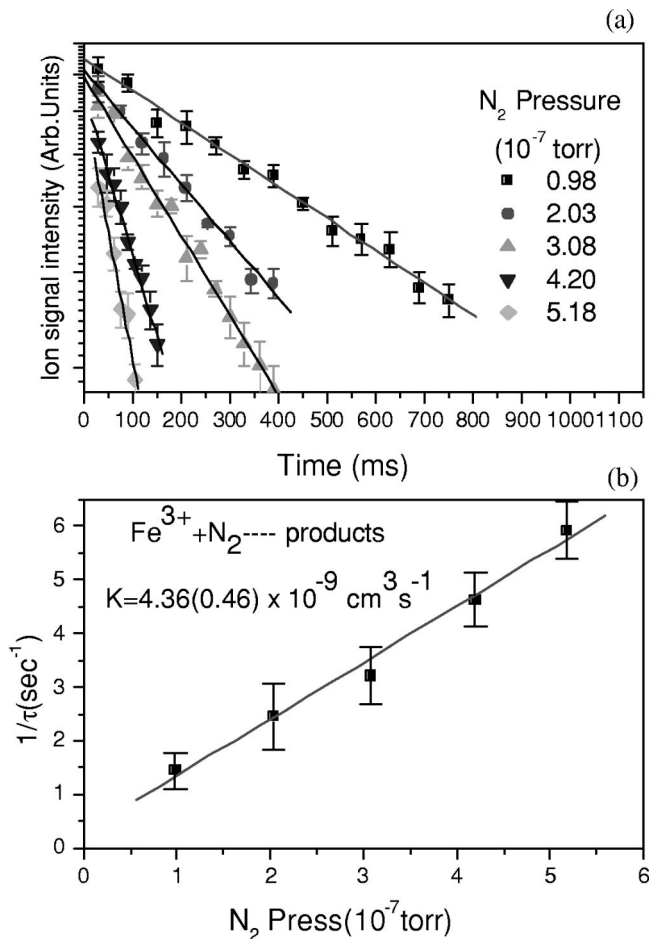
FIG. 4. (a) The decay of relative ion numbers of Fe^{3+} vs storage time in different N_2 pressures. The solid lines are least-square fits to a single exponential function. (b) Variations of the Fe^{3+} decay rate vs N_2 pressure. The slope of the straight line fit gives the charge-transfer rate coefficient.

and then washed with 10^3 torr of the neutral gas. This process is repeated at least five times to minimize contamination of the neutral gas. A variable leak valve (about 10^{-7} torr) controlled the flow rate of the neutral gas. A calibrated nude ionization gauge inside the chamber near the trap assembly is used to measure the gas pressure.

The system is tested and calibrated by measuring the charge-transfer rate coefficient of N^{2+} with N_2, since this work has been done with a similar ion storage technique. Church *et al.* have obtained the rate $2.8(0.6) \times 10^{-9}$ cm^3 s^{-1} ($2-3$ eV) by means of electron bombardment of N_2 in a conventional Penning trap [19]. Fang and Kwong obtained the rate $2.10(0.18) \times 10^{-9}$ cm^3 s^{-1} (2.7 eV) by a laser ablation of solid target TiN [20] in a cylindrical rf Paul trap and $1.73(0.18) \times 10^{-9}$ cm^3 s^{-1} [11] and $2.0(0.2) \times 10^{-9}$ cm^3 s^{-1} (2.7 eV) [20] by electron bombardment of N_2, respectively. In Paul trap by electron bombardment of N_2, we have obtained the charge-transfer rate coefficient of $1.75(0.33) \times 10^{-9}$ cm^3 s^{-1} (2.7 eV). This result is of the same order as the Langevin rate coefficient of 2.6×10^{-9} cm^3 s^{-1} and agrees with earlier measurements (the small difference originates from the different mean collision

energies), which gives us confidence in our next experiment on Fe^{3+} ions.

The Fe^{3+} ions and other ion species are created by laser ablation and are cooled by crossed-beam collisions. The Fe^{3+} ions are selectively stored in the trap by the method mentioned above, and are then extracted from the trap by scanning the rf voltage at a delay time $t_0 + \delta t$ (t_0 refers to the initial delay time, about 50 ms in our measurement) related to the end of the period of selective confinement. Subsequently, these ions are collected by the CEM using the negative potential (about -2600 V in the experiments) applied to the surface of the CEM. The signals from the CEM are amplified by a narrow-banded DC preamplifier and transferred by a fast AD/DA converter, and are recorded by a computer for a later analysis. The charge-transfer rates are determined by measuring the related number of ions stored in the trap as a function of the delay time t after their production under different gaseous pressures. The storage time is scanned from the initial delay time t_0 with a fixed increment δt after each measurement until the ion signal intensity has dropped to one tenth of that at the initial delay time. More than ten such time delay points are used to obtain the data for the analysis. To minimize both the short-term and the long-term ion signal fluctuations and drifts caused by the random changes of laser power and the gradual change of the surface conditions of the target, for each delay time, more than ten data points are collected. Then we repeat such measurements by varying the storage time in the opposite direction. The procedure is then repeated for a number of different gaseous pressures. The average of these data in each time delay gives the mean relative ion density remaining in the trap. To obtain the charge-transfer rate coefficients, we measure the decay rates of the stored ions at five different H_2 or N_2 pressures.

III. RESULTS AND DISCUSSION

Figure 3 is a plot of the reaction $Fe^{3+} + H_2 \rightarrow$ products. Figure 3(a) shows the decay of the relative Fe^{3+} intensity at five different H_2 pressures. The solid line is a least-square fit to the data by a single exponential decay function in a natural logarithmic scale. Referring to $[I(t)/I(t_0)] = e^{-1/\tau}$, its slope $1/\tau$ gives the charge-transfer rate at a given H_2 pressure. Figure 3(b) plots the charge-transfer rate between Fe^{3+} ions and H_2 as a function of H_2 pressures. The solid lines represent the least-squares fit to a linear function of the experimental data. The charge-transfer rate coefficient k is derived from the slope of the ion decay rate $1/\tau$ versus the gas density ρ_r, i.e., $1/\tau = \rho_r k + \Delta_b$, where Δ_b is the interaction rate of Fe^{3+} with the residual gas in the vacuum chamber. For Fe^{3+} ions and H_2 the rate coefficient obtained is $1.64(0.22) \times 10^{-10}$ cm^3 s^{-1}. In the same way, Fig. 4 shows the results of reaction $Fe^{3+} + N_2 \rightarrow$ products. The rate coefficient Fe^{3+} ions with N_2 is $4.36(0.46) \times 10^{-9}$ cm^3 s^{-1}. The uncertainties of the results is mainly due to the statistical fluctuation of the ion signals (typically about 8.6%) and the uncertainty in the estimation of the target gas density (10% for H_2 and 6% for N_2).
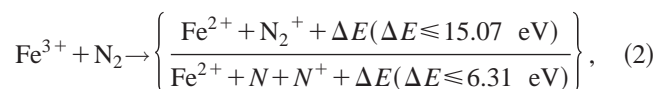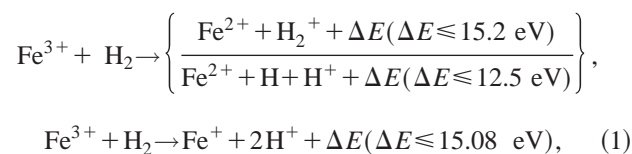
The mean collision energy of the stored Fe^{3+} ions is

about 5.1 eV which is approximately one tenth of the potential well [21,22], the kickout probability of an elastic collision with reactant gas at room temperature (0.04 eV) is very small compared to the axial potential-well depth, and hence this loss process could be ignored in the analysis. This mean energy corresponds roughly to a thermal distribution with the ion temperature of about 4.0×10^4 K. Because the neutral reactant gas is at room temperature (300 K), an equivalent temperature of Fe^{3+} ions with corresponding reaction gas can be obtained from $T_{equiv}/\mu = T_{Fe}/m_{Fe} + T_{gas}/m_{gas}$, where m_{Fe} and m_{gas} are the ion mass and reactant gas mass, respectively, μ is the reduced mass of Fe^{3+} and the reactant gas (i.e., H_2 or N_2), T_{Fe} and T_{gas} are the temperatures of ion and neutral reactant gas, respectively. For Fe^{3+} ions and H_2, the estimated equivalent temperature is about 1.7×10^3 K and that of Fe^{3+} with N_2 is about 1.3×10^4 K. From these data we derive the mean relative velocity between the Fe^{3+} and the reactant gas H_2 or N_2 to be 4.2×10^5 cm/s and 3.8×10^5 cm/s, respectively.

Up to now, no theoretical results or other experimental data have been available at this energy range for charge transfer of Fe^{3+} with neutral atoms or molecules. We have compared the measured results with Langevin cross sections [23]. The static average electric dipole polarizability for H_2 and N_2 is 0.804×10^{-24} cm^3 and 1.74×10^{-24} cm^3, respectively [24]. The corresponding Langevin charge-transfer coefficients for $Fe^{3+} + H_2$ can be estimated to be 8.4×10^{-10} cm^3 s^{-1} and $Fe^{3+} + N_2$ is 1.1×10^{-9} cm^3 s^{-1}. These values are of the same order as our measurements.

The reaction channels with both single and double electrons capture from reaction molecular gas are energetically possible. For example,

$$Fe^{3+} + H_2 \rightarrow \left\{ \begin{array}{l} Fe^{2+} + H_2^+ + \Delta E (\Delta E \leq 15.2 \text{ eV}) \\ \hline Fe^{2+} + H + H^+ + \Delta E (\Delta E \leq 12.5 \text{ eV}) \end{array} \right\},$$

$$Fe^{3+} + H_2 \rightarrow Fe^+ + 2H^+ + \Delta E (\Delta E \leq 15.08 \text{ eV}), \quad (1)$$

$$Fe^{3+} + N_2 \rightarrow \left\{ \begin{array}{l} Fe^{2+} + N_2^+ + \Delta E (\Delta E \leq 15.07 \text{ eV}) \\ \hline Fe^{2+} + N + N^+ + \Delta E (\Delta E \leq 6.31 \text{ eV}) \end{array} \right\}, \quad (2)$$

$$Fe^{3+} + N_2 \rightarrow Fe^+ + 2N^+ + \Delta E (\Delta E \leq 8.0 \text{ eV}),$$

where ΔE is the maximum kinetic energy shared by the ion pairs in their ground states. Since we have not measured the product ion signal for different channels in the experiment, the values we gave are the total charge-transfer rate coefficients of all possible reaction channels.

[1] R. M. Häberli, T. I. Gombosi, D. L. DeZeeuw, M. R. Combi, K. G. Powell, Science **279**, 939 (1997); *Atoms in Astrophysics*, edited by P.G. Burke, W.B. Eissner, D.G. Hummer, and E.C. Percival (Plenum, London, 1983).

[2] Q.D. Wang, E.V. Gotthelf, and C.C. Lang, Nature (London) **415**, 148 (2002).

[3] M. Niimura, I. Cadez, S.J. Smith, and A. Chutjian, Phys. Rev. Lett. **88**, 103201 (2002).

[4] M.S. Pindzola, D.C. Griffrm, S.M. Younger, and H.T. Hanter, Nucl. Fusion Special, Supp. **1**, 21 (1987).

[5] M. Stenke, K. Aichele, U. Hartenfeller, D. Hathiramani, M. Steidl, and E. Salzborn, J. Phys. B **32**, 3627 (1999); M. Stenke, U. Hartenfeller, K. Aichele, D. Hathiramani, M. Steidl, and E. Salzborn, *ibid.* **32**, 3641 (1999).

[6] D.W. Mueller, T.J. Morgan, G.H. Dunn, D.C. Gregory, and D.H. Crandall, Phys. Rev. A **31**, 2905 (1985).

[7] D.C. Gregory, F.W. Meyer, A. Muller, and P. Defrance, Phys. Rev. A **34**, 3657 (1986).

[8] D.C. Gregory, L.J. Wang, F.W. Meyer, and K. Rinn, Phys. Rev. A **35**, 3256 (1987).

[9] J. Linkemann, A. Nuller, J. Kenntner, D. Habs, D. Schwalm, A. Wolf, N.R. Badnell, and M.S. Pindzola, Phys. Rev. Lett. **74**, 4173 (1995).

[10] D.M. Meade, Nucl. Fusion **16**, 289 (1976).

[11] V.H.S. Kwong, T.T. Gibbons, Z. Fang, J. Jiang, H. Knocke, Y. Jiang, B. Ruger, S. Huang, E. Braganza, and W. Clark, Rev. Sci. Instrum. **61**, 1931 (1990).

[12] V.H.S. Kwong, Phys. Rev. A **39**, 4451 (1989).

[13] V.H.S. Kwong, Z. Fang, Y. Jiang, T.T. Gibbons, and L.D. Gardner, Phys. Rev. A **46**, 201 (1992).

[14] M. Yan, M. Feng, K. Gao, and X. Zhu, Chem. Phys. Lett. **289**, 298 (1998).

[15] K. Gao, M. Yan, M. Feng, and X. Zhu, J. Phys. B **35**, 233 (2002); Y. Jiang, Z. Nie, J. Li, and K. Gao, Chin. Phys. Lett. **18**, 528 (2001).

[16] J. Todd, Mass Spectrom. Rev. **10**, 3 (1991).

[17] C. F.Fischer and R.H. Rubin, J. Phys. B **31**, 1657 (1998).

[18] P.T. Rumsby and J.W.M. Paul, Plasma Phys. **16**, 247 (1974); V.H.S. Kwong and Z. Fang, Phys. Rev. Lett. **71**, 4127 (1993).

[19] D.A. Church, and H.M. Holzsheiter, Chem. Phys. Lett. **76**, 109 (1980).

[20] Z. Fang and V.H.S. Kwong, Phys. Rev. A **55**, 440 (1997).

[21] R.A. Heppner, F.L. Walls, W.T. Armstrong, and G.H. Dunn, Phys. Rev. A **13**, 1000 (1976).

[22] D.A. Church and H.G. Dehmelt, J. Appl. Phys. **40**, 3421 (1969).

[23] M.P. Langevin, Ann. Chim. Phys. **5**, 245 (1905).

[24] R.L. David, *CRC Handbook of Chemistry and Physics*, 78th ed. (CRC, Boca Raton, FL, 1997).